

Online Journal of Space Communication

Volume 5
Issue 9 *Global Navigation Satellite System*
(Winter 2006)

Article 26

Receiver Performance for an Enhanced DGPS Data Channel

Gregory Johnson


Michael Kuhn

Peter F. Swaszek

Richard Hartnett

Per Enge

Follow this and additional works at: <https://ohioopen.library.ohio.edu/spacejournal>

 Part of the [Astrodynamics Commons](#), [Navigation, Guidance, Control and Dynamics Commons](#), [Space Vehicles Commons](#), [Systems and Communications Commons](#), and the [Systems Engineering and Multidisciplinary Design Optimization Commons](#)

Recommended Citation

Johnson, Gregory; Kuhn, Michael; Swaszek, Peter F.; Hartnett, Richard; and Enge, Per () "Receiver Performance for an Enhanced DGPS Data Channel," *Online Journal of Space Communication*: Vol. 5 : Iss. 9 , Article 26.

Available at: <https://ohioopen.library.ohio.edu/spacejournal/vol5/iss9/26>

This Article is brought to you for free and open access by the OHIO Open Library Journals at OHIO Open Library. It has been accepted for inclusion in Online Journal of Space Communication by an authorized editor of OHIO Open Library. For more information, please contact debord@ohio.edu.

Receiver Performance for an Enhanced DGPS Data Channel

Gregory Johnson, Michael Kuhn, *Alion Science & Technology, JJMA Marine Sector*

Peter F. Swaszek, *University of Rhode Island*

Richard Hartnett, *U.S. Coast Guard Academy*

Per Enge, *Stanford University*

BIOGRAPHIES

Gregory Johnson is a Senior Program Manager at Alion Science & Technology, JJMA Maritime Sector. He heads up the New London, CT office which provides research and engineering support to the Coast Guard Academy and Coast Guard R&D Center. He has a BSEE from the USCG Academy (1987) a MSEE from Northeastern University (1993) and a PhD in Electrical Engineering from the University of Rhode Island (2005). Dr. Johnson is a member of the Institute of Navigation, the International Loran Association, the Institute of Electrical and Electronics Engineers, and the Armed Forces Communications Electronics Association. He is also a Commander in the Coast Guard Reserves.

Peter F. Swaszek is a Professor of Electrical and Computer Engineering at the University of Rhode Island. He received his Ph.D. in Electrical Engineering from Princeton University. His research interests are in digital signal processing with a focus on digital communications and navigation systems.

Richard Hartnett is Head of the Engineering Department at the U.S. Coast Guard Academy (USCGA). He graduated from USCGA with his BSEE in 1977, and earned his MSEE from Purdue in 1980, and his PhD in EE from University of Rhode Island in 1992. He holds the grade of Captain in the U. S. Coast Guard, and has served on USCGA's faculty since 1985.

Dr. Per Enge is a Professor of Aeronautics and Astronautics at Stanford University, where he is the Kleiner-Perkins, Mayfield, Sequoia Capital Professor in the School of Engineering. He is also the Director of the GPS Research Laboratory, which works with the FAA, U.S. Navy, U.S. Air Force and U.S. Coast Guard to pioneer systems that augment the Global Positioning System (GPS). Per has received the Kepler, Thurlow and Burka Awards from the Institute of Navigation for his work. He is also a Fellow of the ION and the IEEE.

ABSTRACT

The Coast Guard currently operates a maritime differential GPS service consisting of two control centers and over 85 remote broadcast sites. This service broadcasts GPS correction information on marine radiobeacon frequencies to improve the accuracy and integrity of GPS. The existing system provides differential corrections over a medium frequency carrier using minimum shift keying (MSK) as the modulation method. MSK is a version of the Continuous Phase Frequency Shift Keying (CPFSK) modulation technique that is "spectrally compact," meaning that it is a narrow band modulation scheme. In a binary signaling channel, the two instantaneous frequencies for this modulation method are chosen in such a way so as to produce orthogonal signaling with a minimum modulation index. Current DGPS corrections are transmitted at a relatively low data rate, with message structures designed in an era when Selective Availability was in full operation. Greater demands for accuracy coupled with current operations in a "post SA" environment have prompted a reexamination of the DGPS data and signal structure, with an eye towards improving information rate while minimizing legacy user impact.

A two-phased plan for a new generation of DGPS capability can be envisioned. In the first phase (near-term) new ionospheric messages would be introduced to allow greater DGPS accuracy at larger distances from the beacons. This capability could support both double (L1/L2) and triple (L1/L2/L5) frequency operation. This phase requires only the definition of the new message type(s) and the commitment of receiver manufacturers to implement the usage of the new data. In the second phase (intermediate future) a new signal would come on line to support RTK using two and three frequencies and homeland security messaging. This signal would have the capacity to send 500 bps or so without disrupting the legacy signal or legacy receiver performance.

This new signal could be one of the new modulation techniques that we have been investigating; phase trellis

overlay and orthogonal frequency division multiplexing. Preliminary examinations of both of these techniques have shown the potential for increased bandwidth usage (ION NTM Jan. 2004), the effects on legacy receiver performance through a modulator test-bed (ION AM June 2004), and some effects of an actual transmitter (including antenna and coupler) on the signal (ION GNSS Sept 2004). The current paper describes recent investigations into the architecture of the receivers for these modulation methods including details of the demodulation and decoding methods. We also establish receiver performance measures and present preliminary performance results.

INTRODUCTION/eDGPS GOALS

The DGPS system is a medium frequency (MF) radio system that is used worldwide for the broadcast of differential corrections to GPS users. This system adds a digitally modulated signal to transmissions from the marine radio beacons, which operate in the 283.5-325 kHz band. Minimum Shift Keying (MSK) is used to modulate the radio beacon transmissions at data rates of between 25 and 200 bits per second (bps) [1]. MSK is a continuous phase frequency shift keying (CPFSK) modulation technique that is *spectrally compact*, meaning that it occupies minimal bandwidth relative to the bit rate. The U.S. Coast Guard has pioneered this important technology and has provided over ten years of worthy service from the system [2]. Today, the Coast Guard is re-examining the role of DGPS/radio beacons with the goal of optimizing service for the next ten years.

In our earlier papers [3-6] a new generation of DGPS/radio beacon was envisioned in which each radio beacon would be a hybrid datalink capable of accommodating both legacy DGPS signals (at 50, 100, or 200 bps) and new data channels (of 500-1000 bps). The new high data rate channel could be used for RTK style observables, detailed NOAA troposphere and ionosphere models, precise orbit and clock data, or messaging. For these applications, it was envisioned that the system would need to be able to send 500 bps or so without disrupting the legacy signal or legacy receiver performance. The previous papers have examined two approaches:

- Phase Trellis Overlay (PTO): a higher data rate CPFSK phase trellis on top of the existing MSK phase modulation trellis (that passes through the DGPS MSK baud interval phase points) – the result is a constant envelope signal.
- Orthogonal Frequency Division Multiplexing (OFDM): a form of frequency division multiplexing in which adjacent subchannels are themselves narrow and overlapping in frequency. The spectrum is shaped to minimize legacy impact (but the signal is not constant envelope). In our

previous papers we referred to this as Discrete Multi-Tone (DMT) modulation.

The high data rate overlay was first proposed in reference [3]. Reference [4] presented details of both schemes along with theoretical analyses of their performance. Reference [5] examined the co-channel and adjacent channel impacts of the new modulations upon legacy users. This was done both theoretically and experimentally using the modulation test bed. Reference [6] examined the transmitter and antenna effects on the signaling methods and presented prototype receiver architectures.

This paper will address the design, implementation and performance testing of the demodulators for the higher data rate channel using each of the modulation methods.

BRIEF REVIEW OF THE SIGNALING METHODS

We begin with a very brief review of the two approaches: OFDM and PTO. Additional details are available in [4-6].

OFFSET FREQUENCY DIVISION MULTIPLEXING (OFDM) SIGNALING

The concept of parallel transmission of data using frequency subchannels, so called frequency division multiplexing, was developed in the 1960s. In the classical implementation, individual data symbols were modulated over non-overlapping subchannels so as to avoid interchannel interference (in some cases, guard bands were added to decrease the possibility of interference). Unfortunately, such an approach is spectrally inefficient. To improve matters, OFDM allows the subchannels to overlap, but uses orthogonal subcarriers for each so as to avoid interference [7]. Specifically, for a symbol duration of T seconds, the subchannels are spaced by $1/T$ in frequency. OFDM can be implemented by a bank of modulators, one for each subchannel. It is also possible to employ Fast Fourier Transform techniques to convert the problem into one of baseband modulation, taking an inverse FFT (IFFT) followed by standard modulation.

In the frequency domain, OFDM appears to consist of a collection of closely spaced, overlapping subchannels. By selectively turning individual channels on or off (i.e. not modulating them), the spectrum of the entire OFDM signal can be controlled. Viewed in the time domain, OFDM is essentially pulse amplitude modulation of a correlated data stream (correlated by the IFFT operation). For our eDGPS transmission, OFDM is added to the legacy MSK.

For the OFDM approach, we assume a standard MSK transmission at 50 bps (this yields a much narrower legacy spectrum, offering more room for OFDM data rate). Currently we have implemented OFDM using $N=16$ subchannels, using a QAM16 signal constellation on each

(see [4, 8] for details). We set the OFDM signaling rate at 500 symbols/sec (sps) in order to place spectral nulls at adjacent MSK channel frequencies. We zero out the 4 center subchannels to get a spectral notch near the legacy MSK. Running at a raw bit rate of 1000 bps, this gives us an effective bit rate of 750 bps. The entire system has not been optimized yet, so some of these parameters are subject to change in the future. This however, is what we are currently using for testing (see Figure 1).

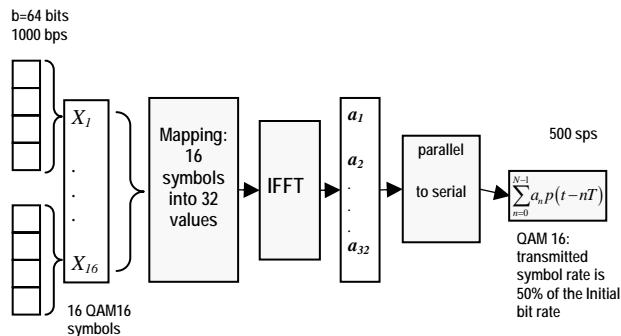


Figure 1 – N=16, QAM16, 1000 bps OFDM, block diagram.

The theoretical spectrum for our N=16 OFDM signal is shown in Figures 2 and 3. In each case, the blue line is the spectrum for all 16 channels being modulated; the green line is the spectrum that results if we assume that sub-channels 1, 2, 3 and 16 are turned off. With no power in these four center subchannels, the spectrum has a notch around the legacy pass bands shown in dashed black. The legacy MSK spectrum is shown in solid black. As shown in Figures 2 and 3, the high-rate OFDM power spectral density drops to below -36 dBW/Hz across the legacy pass bands. The spectrum also has deep nulls at ±500 Hz, thus protecting adjacent channels. The spectrum is much wider bandwidth than the legacy MSK however.

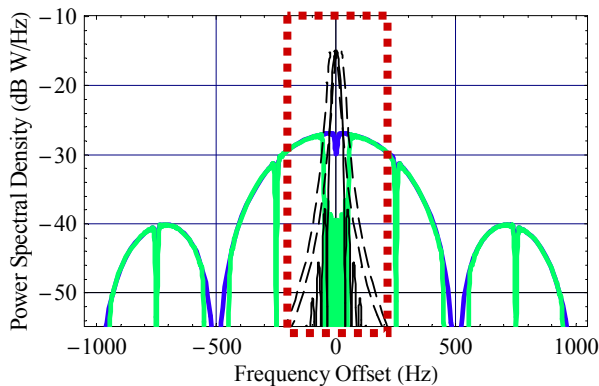


Figure 2 – 500 sps, N=16 OFDM theoretical spectrum.

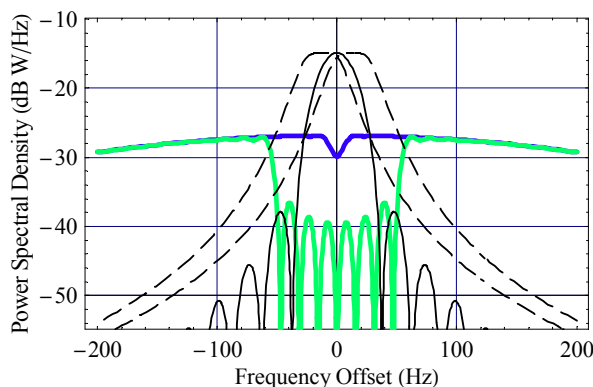


Figure 3 – A closer look at N=16 OFDM (the red box of Figure 2).

REVIEW OF MSK

From Pasupathy [9] we can write an MSK signal as

$$s(t) = a_I(t) \cos \frac{\pi t}{2T} \cos 2\pi f_c t + a_Q(t) \sin \frac{\pi t}{2T} \sin 2\pi f_c t$$

in which $a_I(t)$ and $a_Q(t)$ are alternating bit pulses (each a rectangular pulse of value ± 1 and duration $2T$ centered on the start of the bit time kT for bit a_k , i.e. $(k-1)T \leq t \leq (k+1)T$) which truncate the cosine or sine envelope terms. This is shown in Figure 4:

- The first subplot shows the *in-phase*, or even bits, with the cosine envelope for $2T$ seconds – notice that $a_Q(t) = +1$ creates a single positive half-wave of a sinusoid from $-T$ to T .
- The second subplot shows the *quadrature*, or odd bits, with the sine envelope for $2T$ seconds – notice that $a_k(t) = +1$ creates a single positive half-wave of a sinusoid from 0 to $2T$.
- The third subplot shows the resulting sum with the cosine and sine modulations, respectively.

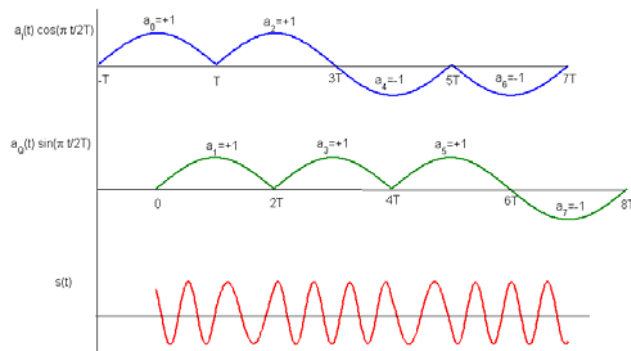


Figure 4 - Pictorial Explanation of MSK.

A primary attractiveness of this view of MSK is its appearance as two bit streams (antipodal signaling with bit duration $2T$) on two orthogonal modulations.

The optimum receiver for MSK in AWGN is simple due to the orthogonality of the cosine and sine carrier modulations. As shown in Figure 5, the demodulator consists of separate even and odd bit demodulators on the

I and Q channels, each a correlator or matched filter to a modulated half-wave of a cosine pulse of time duration $2T$.

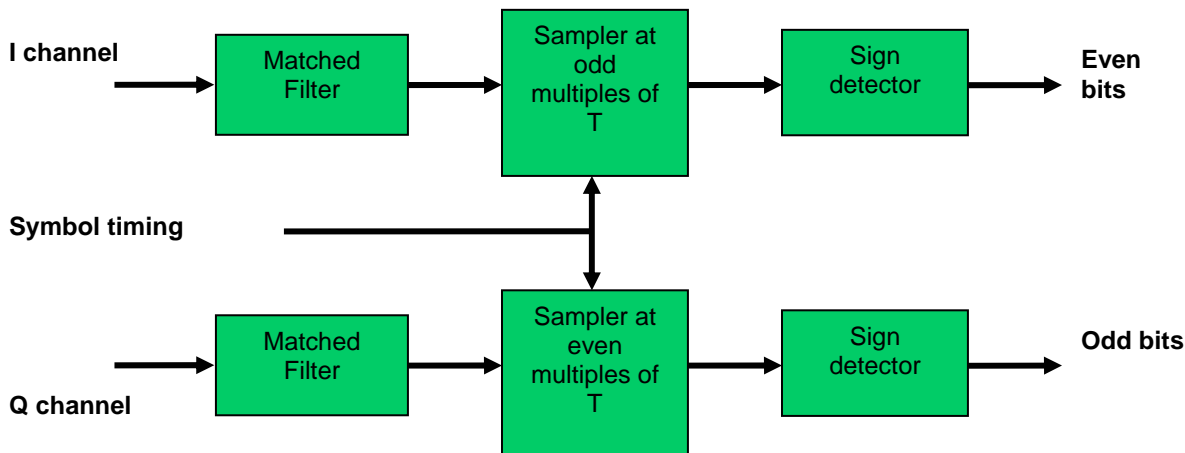


Figure 5 – MSK Demodulator.

Depending upon the values of adjacent (even and odd) bits, we can apply a trigonometric identity to get a continuous phase form for MSK. Specifically, since $a_I(t)$ and $a_Q(t)$ both equal ± 1 , use of

$$\cos \alpha \cos \beta \pm \sin \alpha \sin \beta = \cos(\alpha \mp \beta)$$

allows MSK to be written as

$$s(t) = \cos \left[2\pi f_c t + \frac{\pi t}{2T} b_k(t) + \phi_k \right]$$

in which $b_k(t) = -a_I(t)a_Q(t)$ and ϕ_k equals either 0 or π . In this form, $b_k(t)$ tells the direction of the phase shift over the period (equivalently, the value of the frequency shift) and ϕ_k is the starting phase for the even bit period. A common visual representation for this form of MSK is a phase diagram or, since the adjacent phase shifts are 90° per bit interval due to the modulation index being equal to $1/2$, a phase trellis. This phase diagram and trellis are shown in Figures 6 and 7, respectively. In both figures, the horizontal axis is time with horizontal spacing between adjacent circles equal to the bit interval T . The vertical axis is phase with vertically adjacent circles being 180° apart; the full set of phase values at the bit interval endpoints range through 90° steps.

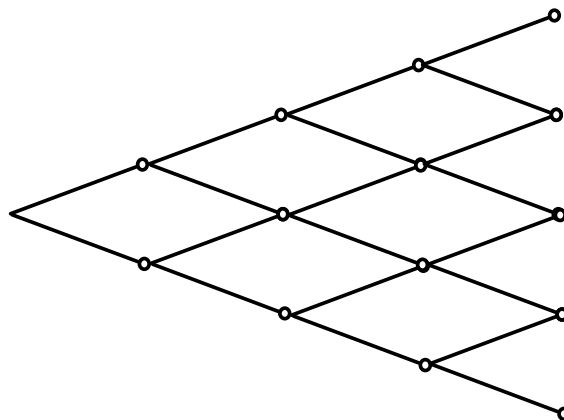


Figure 6 – Traditional MSK Phase Diagram

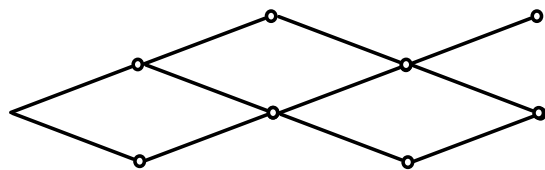


Figure 7 – Traditional MSK Phase Trellis.

PHASE TRELLIS OVERLAY (PTO) – JAN. 2004 METHOD

First, we review the method detailed in our January 2004 ION paper [4]. From above, a standard MSK signal is of the form

$$s(t) = \cos \left[2\pi f_c t + \frac{\pi t}{2T} b_k(t) + \phi_k \right]$$

To more explicitly show the impact of the entire bit sequence, we write this as

$$s(t, \bar{a}) = \cos[2\pi f_c t + \phi(t, \bar{a})]$$

in which the phase $\phi(t, \bar{a})$ depends upon the data sequence \bar{a} and follows a continuous trajectory through a trellis as shown in Figure 7.

The concept of the phase trellis overlay approach is to add additional phase paths to the phase diagram/trellis. Specifically, we constrain the phase to go through the same set of phase values at the ends of each bit period, but allow different trajectories between each. For example, Figures 8 and 9 show a phase tree diagram and trellis, respectively, with double the bit rate of MSK; the extra bit per interval determines which parallel phase path to take. Clearly additional paths could be added to further increase the data rate. Our view is that the set of circles (or phase values every T seconds) traversed through this augmented diagram/trellis will be the same as those determined by the original MSK transmission; the actual paths to go from circle to circle will vary depending upon additional data bits (hence, the use of the work “overlay”).

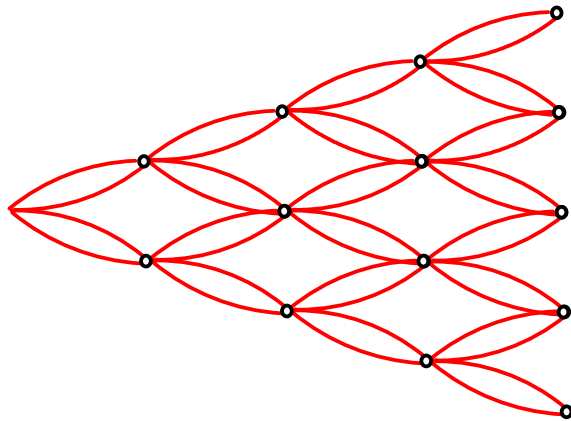


Figure 8 – Double the Rate Phase Diagram.

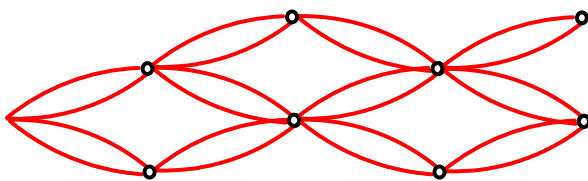


Figure 9 – Double the Rate Phase Trellis.

We have done further examination of this approach: computing the resulting spectrum, developing efficient path sets, and examining the ability of DGPS transmitters to modulate the resulting waveform. These results are described in a June 2004 ION paper [5]. Figure 10 shows

a typical trellis considered; in this case, 8 paths per bit interval (or 2 extra bits per T seconds). We note that this example is a true sub-trellis of the original MSK in that the paths themselves form a trellis. In this figure the traditional MSK phase path is shown in blue.

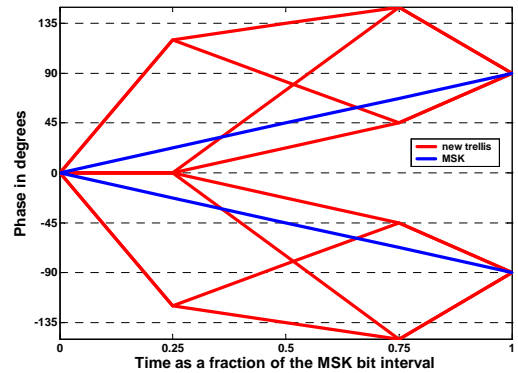


Figure 10 – 8 Path Overlay Modulation – rate tripling MSK.

The purpose of the current work is to examine receiver issues. The optimum receiver for this modulation consists of a Viterbi decoder; to date we have implemented a finite delay decoder, but drop this method for the time being to further explore a related modulation scheme with simpler demodulator.

HIGHER RATE MSK (HR-MSK)

Recall the in-phase/quadrature expression for MSK

$$s(t) = a_I(t) \cos \frac{\pi t}{2T} \cos 2\pi f_c t + a_Q(t) \sin \frac{\pi t}{2T} \sin 2\pi f_c t$$

In this expression, both $a_I(t)$ and $a_Q(t)$ are rectangular pulses of value ± 1 and duration $2T$ which represent the MSK data. The cosine and sine terms (with arguments $\frac{\pi t}{2T}$) can be thought of as convenient pulse shapes that allow the use of a trigonometric identity to result in a constant amplitude, continuous phase sinusoid. Now, let’s allow more general waveform shapes $g_I(t)$ and $g_Q(t)$, but still time limited to $[0, 2T]$.

$$s(t) = a_I(t)g_I(t) \cos 2\pi f_c t + a_Q(t)g_Q(t) \sin 2\pi f_c t$$

Clearly, many different pulse shapes could be used here. Prior research [10] has considered this idea (so called *generalized MSK*) for improving the spectrum of MSK while maintaining the constant amplitude property and the phase values at the bit interval endpoints.

Instead, here we propose using different pulse shapes to convey additional data. Our approach, much like Simon’s,

is to imagine that $g_I(t)$ and $g_Q(t)$ are still sinusoidal, but to vary the phase rate of change in different ways

$$g_I(t) = \cos\theta_k(t) \quad g_Q(t) = \sin\theta_k(t)$$

One example, that would double the data rate of the transmission, is shown in Figure 11. This figure shows a $2T$ interval, corresponding to a pulse on the I or Q channel. The upper subfigure shows the phase $\theta_k(t)$ of the pulse shape (blue is the linear phase in traditional MSK, the two red curves are two possible phase trajectories for the double rate MSK extension – in this example they are a linear phase plus or minus a sinusoid of amplitude 30°). The lower subfigure shows the actual pulse shapes.

One note on such a method is that the resulting combination of the I and Q channels is no longer a constant amplitude sinusoid. Nor does it generally pass through the phase values of multiples of 90° at the bit intervals. Proper restriction of the form of the phase functions could cause this latter condition. For example, Figure 12 shows two pulse shapes (red and green) that would cause the resulting signal to have the usual MSK phase at the bit interval boundaries.

At the moment, though, we will not concentrate on the constraint of constant amplitude, and will examine the performance of a rate tripling modification (i.e. 4 distinct pulse shapes to add 2 bits per bit interval). These 4 pulse shapes are shown in red in Figure 13 for comparison to the original MSK pulse (in blue). Experimental examination suggests that these pulse shapes have a minor impact on the spectrum of the MSK signal (compare the spectra of typical modulations shown in Figures 14 and 15). Further, the clear positive nature of the pulse implies little impact on performance of a legacy MSK receiver.

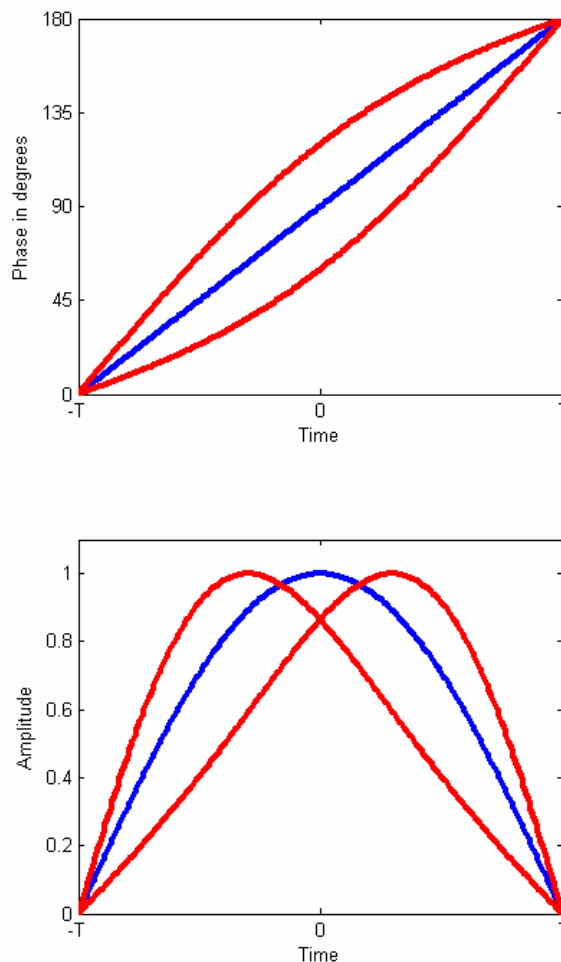


Figure 11 – Possible pulse shapes for higher rate MSK: blue is MSK and red is a 2 bit per interval modification.

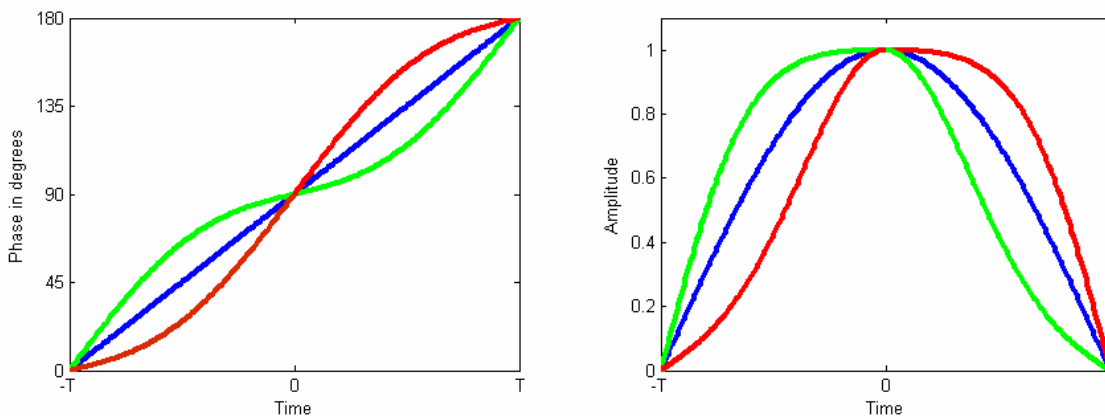


Figure 12 – Sample phase functions that achieve the MSK bit interval phases.

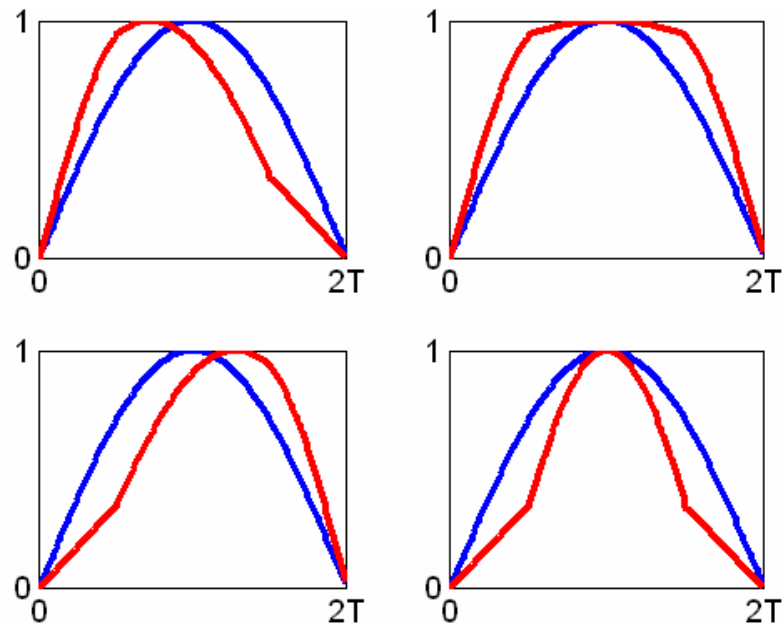


Figure 13 – Rate tripling HR-MSK.

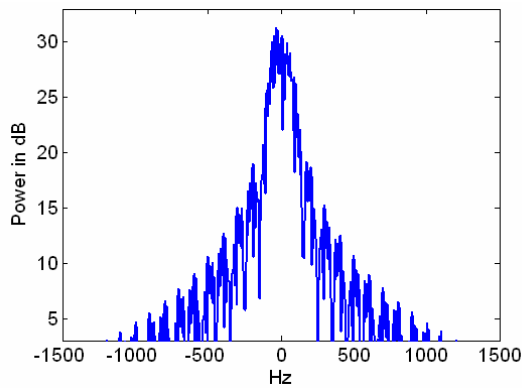


Figure 14 – MSK Spectrum

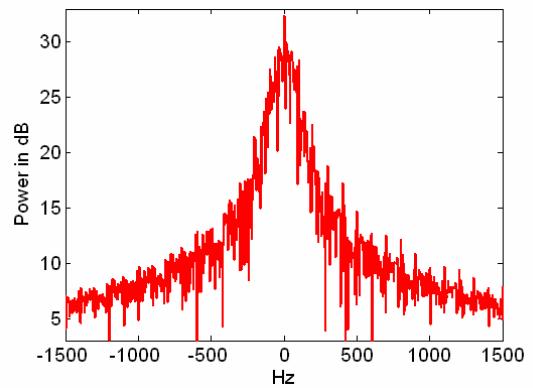


Figure 15 – New HR-MSK Spectrum

DEMODULATORS

The majority of the current work has been to develop the demodulators for each of the modulation techniques and then use them to conduct performance testing. Each receiver design and details on the demodulator will be discussed in the following sections.

OFDM DEMODULATOR

The OFDM receiver architecture is shown in Figure 16. As is typical with a software receiver the goal was to get the A/D converter as close to the antenna as possible. An analog front-end is needed to provide bandpass filtering and gain prior to the A/D but this is the only component between the antenna and the A/D. Once the RF is digitized all operations are done digitally. The signal is brought to baseband using I & Q downconversion. Carrier phase and symbol period tracking is done to keep the

receiver synchronized both to the carrier frequency and to keep the symbols aligned. At this point the data demodulation can be done – of both the low rate (MSK) and high rate (OFDM) bits.

A detailed schematic of the demodulator is shown in Figure 17. The demodulator, which has been implemented in MATLAB™ works on digital I and Q data where the symbol periods have been identified and synchronized with. The OFDM signal being an amplitude modulation is carried on only the inphase channel (I). MSK being a phase modulation is carried on both the inphase (I) and quadrature (Q) channels. Both the I and Q channels are thus used to demodulate the legacy MSK using a matched filter on the complex data (I-jQ). This yields the low rate data at 50bps.

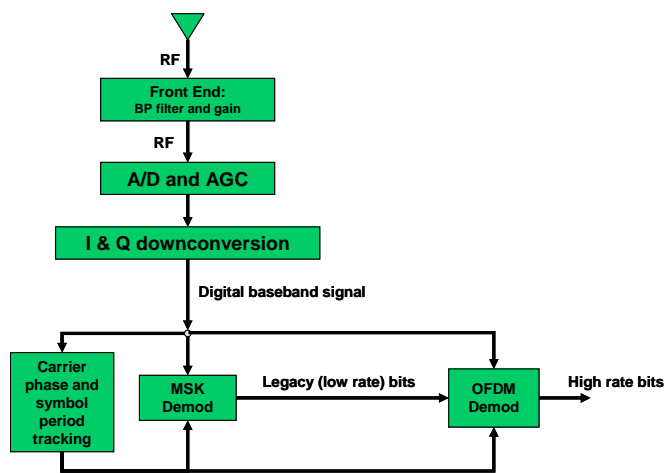


Figure 16 – OFDM Receiver Design

Since the inphase (I) channel has both the OFDM and the MSK, we need to remove the MSK in order to

demodulate the OFDM signal. The I channel is low-pass filtered to help with adjacent channel rejection. The demodulated MSK bits are used to regenerate the inphase channel of the MSK which is subtracted from the I channel to leave just the OFDM signal. The OFDM symbols are determined by detecting the amplitudes of the square pulses in each high-rate symbol period.

The symbol values (amplitudes) are then processed in reverse of what was described earlier for the modulator. A block of 32 symbols is collected. These are converted into 32 complex values using the FFT operation. The 16 complex QAM “symbols” are obtained by an unmapping operation from the 32 complex values. These are fed into a QAM16 demodulator to return the 64 bits corresponding to the 16 QAM16 symbols. Some of these bits are null bits because they correspond to channels that were zeroed out at the transmitter so they are removed; leaving 48 bits. Feeding the demodulator at the 500 symbols/second returns the effective bit rate of 750 bps.

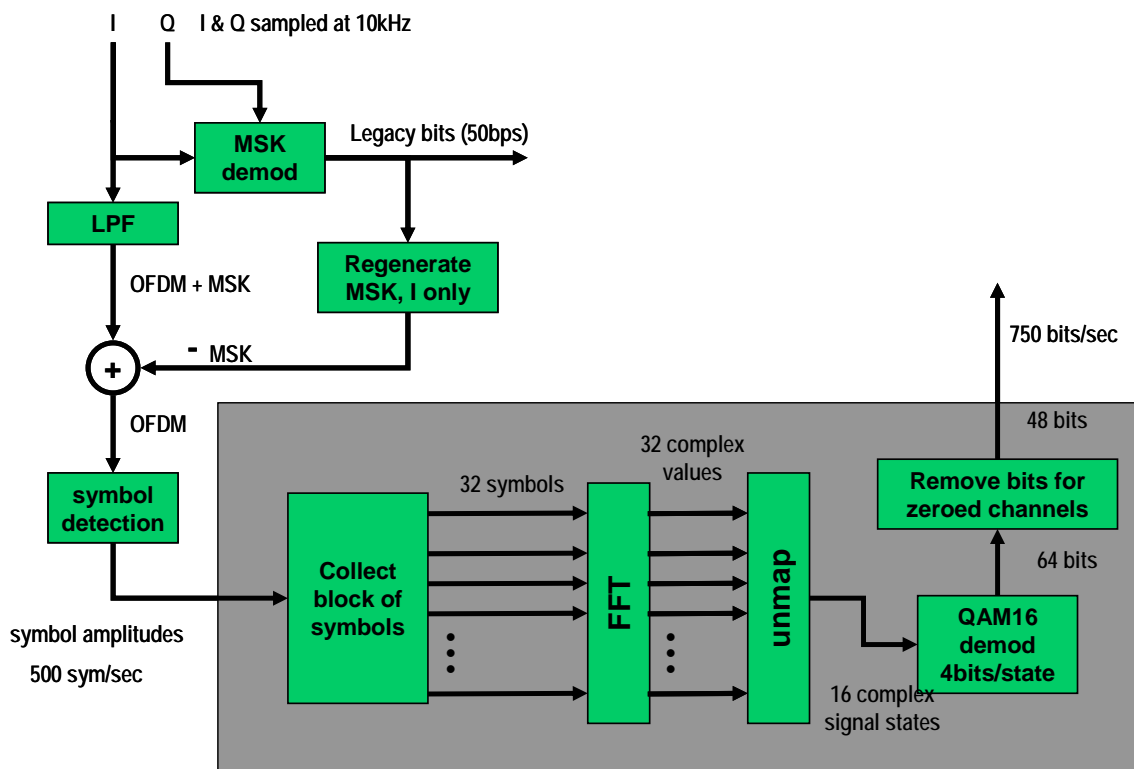


Figure 17 – OFDM Demodulator

The time domain representation of the OFDM signal is shown in Figure 18. The combination of the OFDM and MSK signals can be seen on the inphase channel (magenta); the MSK signal alone is seen on the quadrature channel (cyan). The reconstructed inphase MSK is shown in green. This is the signal that is removed from I to leave just the OFDM signal (shown in black). The red stars are the amplitude levels determined by the symbol detection.

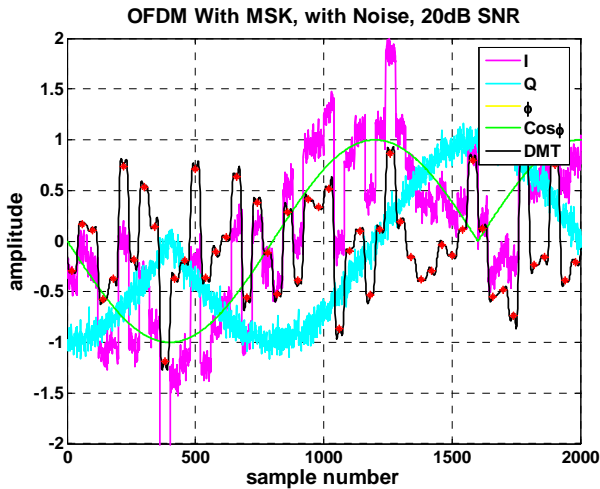


Figure 18 – Time Domain Representation of OFDM Signal

The operation of the QAM16 demodulator is shown in Figure 19. Here the complex QAM16 symbols are shown as they map to the QAM16 signal constellation of +/-1 and +/-3. The cluster of points in the center (0) which would not be there for normal QAM16 modulation correspond to the channels that were zeroed out to make the spectral notch.

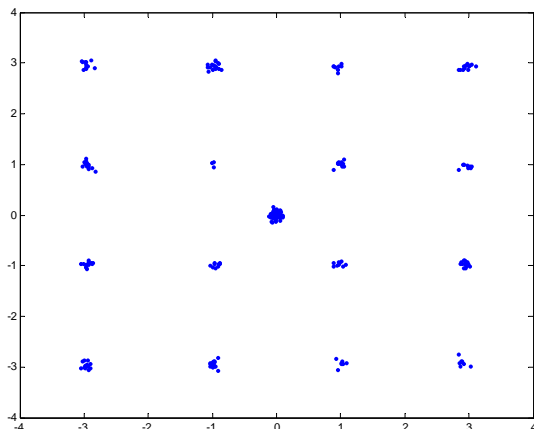


Figure 19 – QAM16 Signal Constellation

HR-MSK DEMODULATOR

The HR-MSK receiver architecture is shown in Figure 20. This receiver architecture is very similar to the OFDM receiver; the only difference is the demodulator. In this case a single demodulator will yield both low and high rate bits.

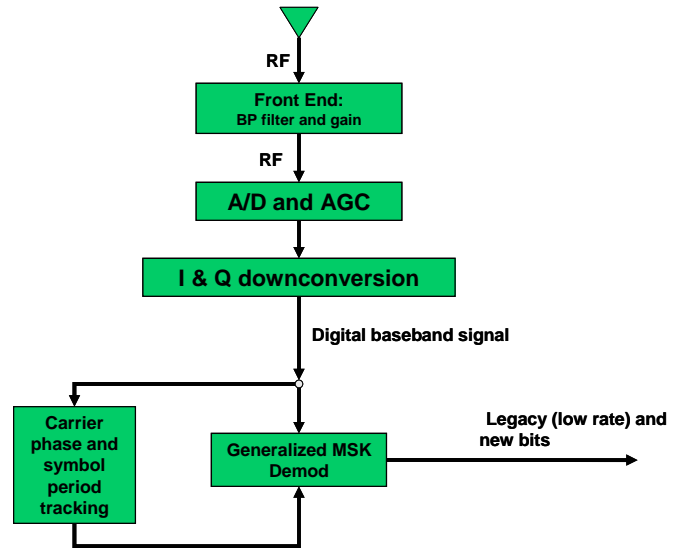


Figure 20 – PTO Receiver

Since HR-MSK still consists of parallel I and Q channels, the matched filter/correlator receiver of Figure 5, with parallel channels for each I and Q, is still optimum. What changes is that each channel has a bank of matched filters as shown in Figure 21, one for each pulse shape. Of the results from these matched filters, the largest one (in absolute value) is identified as the pulse sent due to the additional bits; the sign of this value determines the legacy MSK bit.

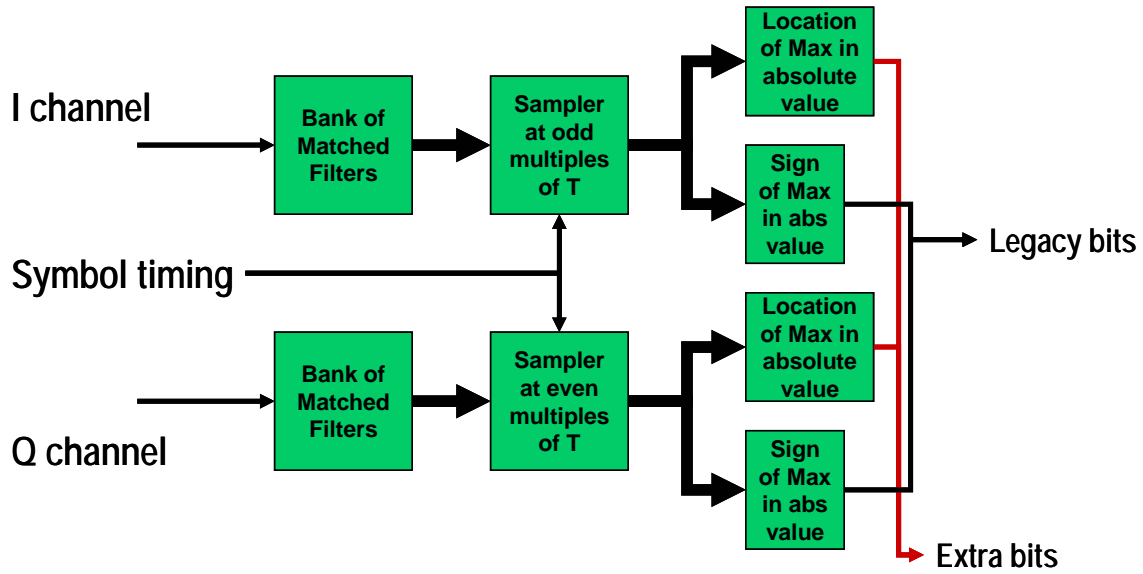


Figure 21 – PTO Demodulator

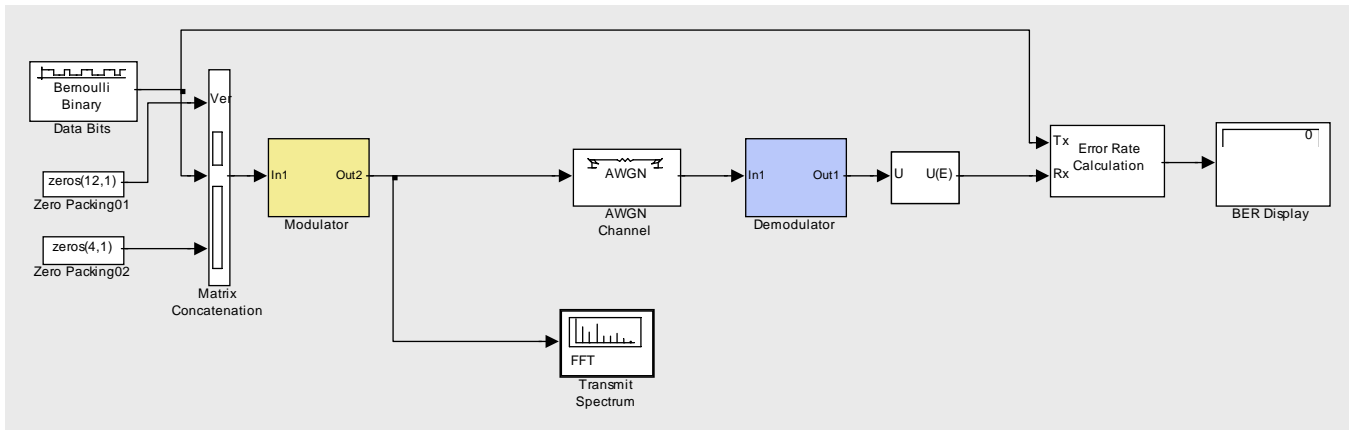


Figure 22 – SIMULINK™ Model of OFDM System

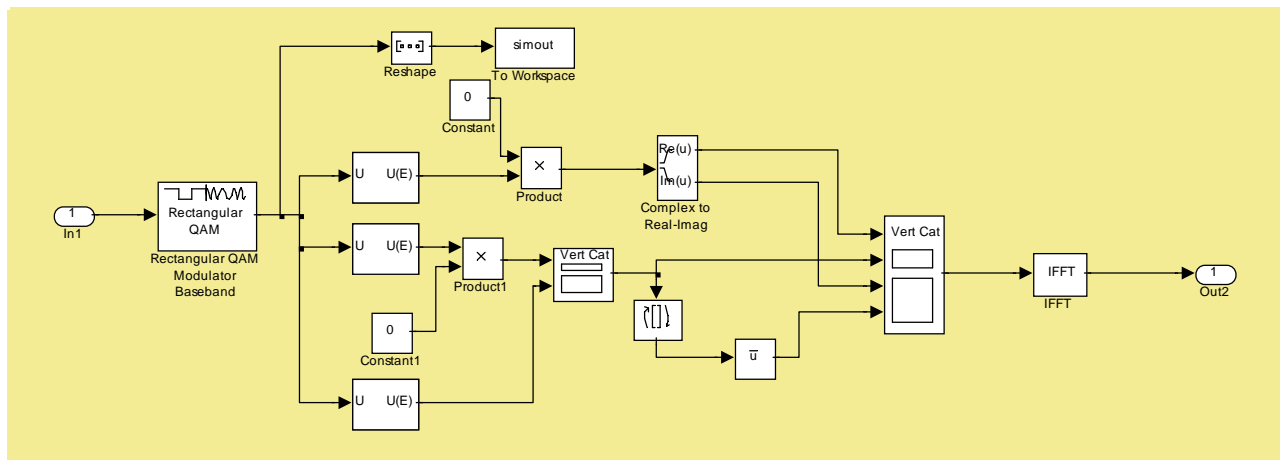


Figure 23 – OFDM Modulator Block

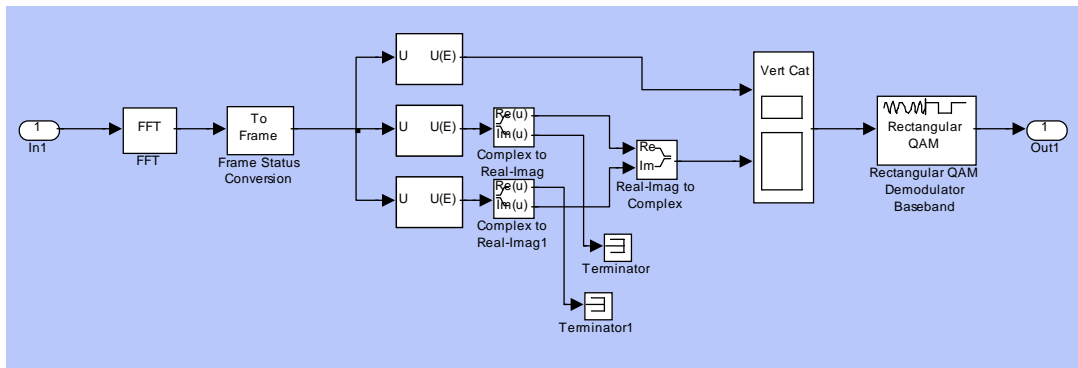


Figure 24 – OFDM Demodulator Block

SAMPLE PERFORMANCE

The performance of these two modulation techniques has been examined. SIMULINK models of the systems have been implemented to assist in the performance examination; the OFDM SIMULINK model is shown in Figures 22 – 24. In addition, end-to-end testing of the MATLAB modulators-demodulators has been conducted as shown in Figure 25. Random bits are generated for both the low and high data rate channels. The signal is generated (both low and high rate) and the digital RF (at baseband) is streamed continuously to files (~1sec/file). In order to measure low Bit Error Rates (BER) a large number of bits must be transmitted (at least 10 times the reciprocal of the BER to be measured); thus the testing must be done for a fairly long time period (10,000 files were generated, about 2.7 hrs of continuous data). The demodulator would then read the digital RF continuously from files, add noise (various noise levels were used in order to plot BER vs. SNR), and then demodulate both data streams (low and high rate). The output bits were compared to the stored input bits in order to calculate errors and compute BER.

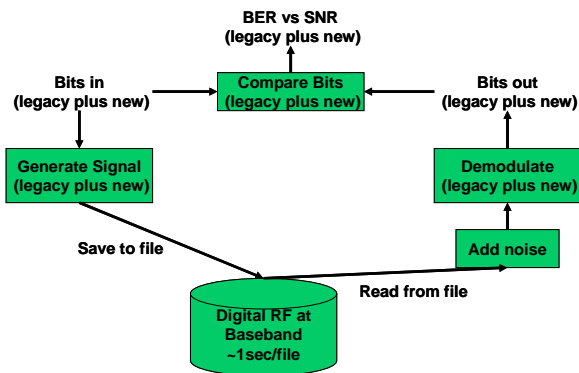


Figure 25 – System Simulation

A plot of the BER vs. SNR for the OFDM&MSK system is shown in Figure 26. The baseline MSK-only signal is shown in green. The impact on MSK (legacy signal) of transmitting the OFDM overlay is about 1dB as shown by the red curve. The OFDM signal (the blue curve) requires about 22dB greater SNR compared to that of the MSK to achieve the same BER. This is understandable given that the MSK is at 50bps and the OFDM is at 750bps with both modulations occurring at equal power levels.

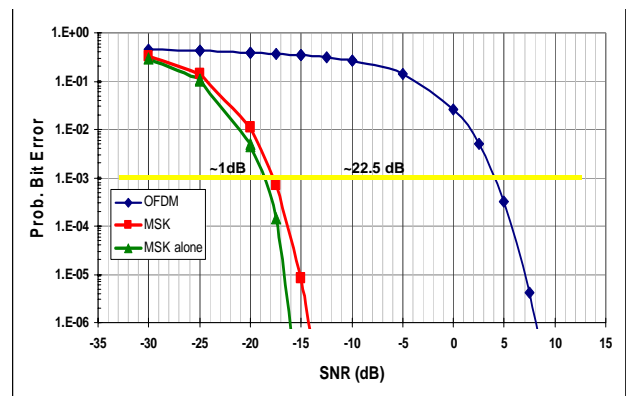


Figure 26 – BER vs. SNR for OFDM & MSK

A similar plot for the PTO&MSK system is shown in Figure 27. Again the legacy MSK-only is shown in green and the impact on the legacy MSK performance of the high rate overlay is about 1dB (in signal space, the legacy component of the new HR-MSK signals are slightly closer together under antipodal signaling – for the moment we have not doubled the transmitted power as we do for OFDM above, otherwise the legacy component would have improved by about 2 dB). The high rate component only requires about 16.5dB greater SNR for equivalent performance – though this high rate system is only running at an additional 400 bps (versus 750 for OFDM) and higher rates need to be examined.

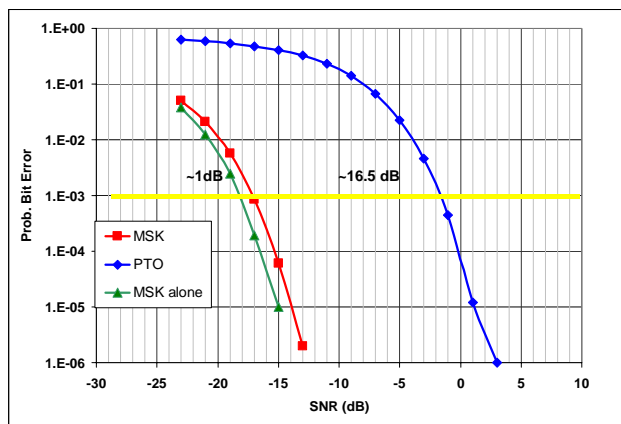


Figure 27 – BER vs. SNR for PTO & MSK

We also investigated the impact of an MSK signal in the adjacent channel. In previous work [5], we had investigated the impact of the new modulations on the legacy MSK in the adjacent channel. Here we investigated the impact of the adjacent channel on the high rate system. Two cases were examined; having an adjacent channel (+1000 Hz) MSK signal at equal power (Figure 28) and having the adjacent channel MSK signal at +36dB (Figure 29).

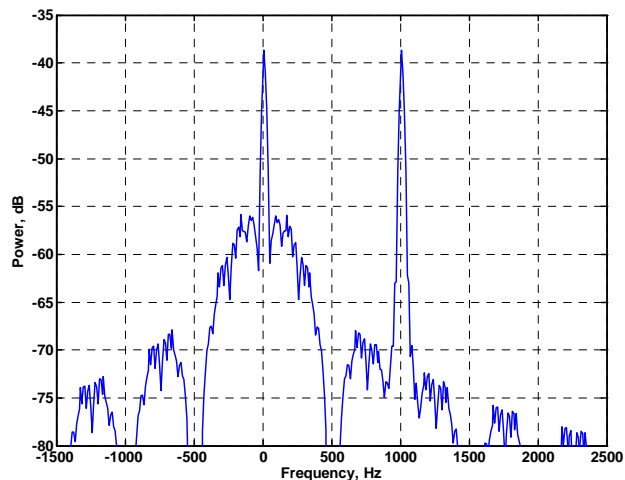


Figure 28 – OFDM Spectrum with Adjacent Channel at Equal Power

For the OFDM system, the results are shown in Figure 30. Here the system breaks down totally with the 36dB stronger signal in the adjacent channel, under the current implementation. With the adjacent channel at equal power, the impact is about a 2.5 dB loss in performance. This performance could perhaps be improved through better filtering and/or pulse shaping of the OFDM pulses. As a comparison, Figure 31 shows the adjacent channel impact on the legacy MSK signal. These curves are for MSK-only being transmitted. Here the legacy MSK suffers a 35dB loss due to the +36dB adjacent channel

signal and a 3dB loss for the equal power case. What level of adjacent channel interference is realistic and must be accounted for is thus being investigated.

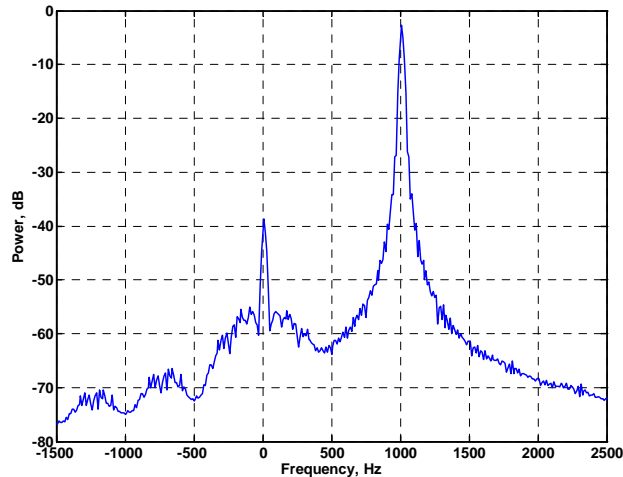


Figure 29 – OFDM Spectrum with Adjacent Channel at +36dB.

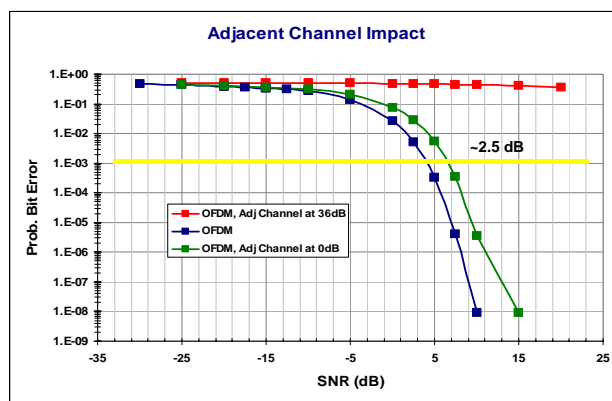


Figure 30 – Adjacent Channel Performance, OFDM

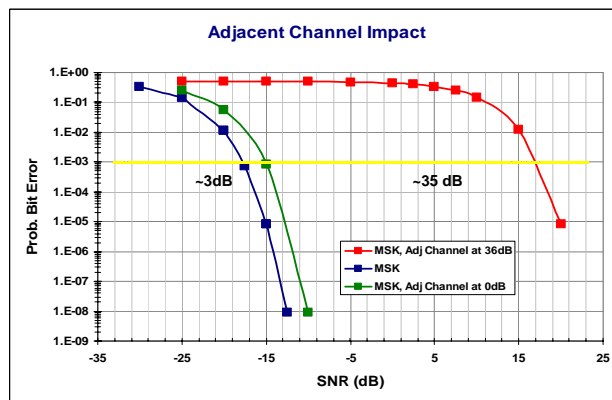


Figure 31 – Adjacent Channel Performance, MSK.

We also simulated HR-MSK with an adjacent channel MSK signal (1 kHz away in center frequency) to see the impact of adjacent channels on HR-MSK performance. The results of the simulation are indistinguishable from the data in Figure 27 so are not included in this treatment.

CONCLUSIONS / FUTURE

The Advanced Modulation Testbed has been implemented. We have developed software receivers for the OFDM and PTO (including new HR-MSK) concepts. These receivers will allow us to further examine the impacts of choices made in the implementation of the modulation methods:

- OFDM – data rate and data block size, subchannel usage, signal constellation, pulse shape, relative power level of MSK and OFDM
- PTO/HR-MSK – data rate, pulse shapes, phase trajectories

Further, we will be able to better test the impact of channel interference, including typically expected noise levels and adjacent channel effects. This has impacts on the frequency reuse system-wide.

Future work on completing the receivers is adding the capability to do carrier synchronization (both frequency and phase) and bit timing recovery. In the future we will examine the effectiveness of using Forward Error Correction (FEC) techniques and we will also examine the impact on the high rate demodulation performance of band limiting the transmission.

ACKNOWLEDGEMENTS

This work has been made possible through the support of the sponsors, Mr. Dave Wolfe, Mr. Al Cleveland and Mr. Mike Parsons at Coast Guard Command and Control Engineering Center (C2CEN). The authors also acknowledge the coding assistance provided by Ken Dykstra of Alion Science & Technology.

DISCLAIMER AND NOTE

The views expressed herein are those of the authors and are not to be construed as official or reflecting the views of the Commandant, the U.S. Coast Guard, or any agency of the U.S. Government.

REFERENCES

- [1] "Technical Characteristics of Differential Transmissions for Global Navigation Satellite Systems from Maritime Radio Beacons in the Frequency Band 283.5 - 315 kHz in Region 1 and 285 - 325 kHz in Regions 2 and 3," International Telecommunications Union ITU-R M.823-2, 1997.
- [2] "Differential Global Positioning System (DGPS) Navigation Service Concept of Operations," U.S. Coast Guard, Washington, DC Commandant Instruction 16577.2, 16 August 1995.
- [3] R. Hartnett, K. Gross, B. Bovee, S. Nassar, G. Johnson, G. Sanders, P. Swaszek, and D. Wolfe, "DGPS Accuracy Observations and Potential Data Channel Improvements," presented at Fifty-ninth Annual Meeting, Institute of Navigation, Albuquerque, NM, 23-25 June, 2003.
- [4] R. Hartnett, K. Gross, M. McKaughan, P. Enge, P. Swaszek, G. Johnson, A. Cleveland, and M. Parsons, "Novel Signal Designs for Improved Data Capacity from DGPS Radiobeacons," presented at Institute of Navigation, National Technical Meeting, San Diego, CA, 26-28 January, 2004.
- [5] P. Swaszek, R. Hartnett, P. Enge, G. Johnson, and K. Gross, "Performance of Signal Designs for Improved Data Capacity from DGPS Radio Beacons," presented at Institute of Navigation, Annual Meeting, Dayton, OH, 6 - 9 June, 2004.
- [6] G. Johnson, P. Swaszek, R. Hartnett, and P. Enge, "Transmitter Effects and Receiver Prototyping for Improved Data Capacity from DGPS Radiobeacons," presented at Institute of Navigation GNSS, Long Beach, CA, 21-24 Sep 2004.
- [7] A. L. Intini, "Orthogonal Frequency Division Multiplexing for Wireless Networks," Univ. of Calif. Santa Barbara, Technical Report December 2000.
- [8] J. M. Cioffi, "A Multicarrier Primer," Amati Communications Corp. and Stanford University, Palo Alto, CA 1991.
- [9] S. Pasupathy, "Minimum Shift Keying: A Spectrally Efficient Modulation," *IEEE Communications Magazine*, vol. 17, pp. 14-22, 1979.
- [10] M. K. Simon, "A Generalization of Minimum-Shift-Keying (MSK)-Type Signaling Based Upon Input Data Symbol Pulse Shaping," *IEEE Transactions on Communications*, vol. COM-24, pp. 845-856, 1976.